International Research Journal of Engineering and Technology (IRJET) e-ISSN: 2395-0056
Volume: 07 Issue: 12 | Dec 2020 www.irjet.net p-ISSN: 2395-0072

STABILITY ENHANCEMENT OF DOUBLY FED INDUCTION GENERATOR WITH VIRTUAL RESISTANCE UNDER NETWORK DISTURBANCES

S. Rajesh[a*], Dr. P. Venkata Prasad[b], Dr. P. Srinivas[c]

[a]Research Scholar, Dept. of Electrical Engineeing, University college of Engineering, Osmaina University, Hyderabad, Telangana state, India, 500007*
[b]Professor, Dept. of Electrical & Eletronics Engineeing, Chaithanya Bharathi Institute of Technology, Gandipet, Hyderabad, Telangana state India, 500075
[C]Professor, Dept. of Electrical Engineeing, University college of Engineering, Osmaina University Hyderabad, Telangana state, India, 500007

Abstract: In olden days the grid stability can be maintained by crowbars but this method has few considerable limitations. In this paper a new technique dynamic virtual resistance control strategy is proposed for the case of over current on the rotor side converter of the DFIG under grid faults. In order to fulfill the requirements of reactive power in wind farms the crowbars are not preferable because they absorb the reactive power from grid whereas virtual resistance system supplies the reactive power to the grid. This control method can suppress the oscillations of the current component on the rotor side and improves the transient stability of the DFIG. The resistance of the virtual resistor will change with the voltage drop and it can better meet the synergistic suppression of the rotor side converter electrical stress under different conditions. Hence this paper in order to maintain stability of DFIG, first transient mathematical models of doubly fed induction generator under grid voltage symmetrical drops are established, and a modified control strategy is developed with virtual resistance then analyze the transient characteristics of it.

Keywords: Crow bar circuit, DFIG (Doubly Fed Induction Generator), Virtual Resistance.

1. Introduction:

The wind power energy technology has developed rapidly due to its clean and pollution free nature. It also does not produces green house gases, occupies less area on the land and its maintenance is also very less. In the variable speed constant frequency wind power generation system, the DFIG is widely used due to its advantages of small converter capacity, independent control of active power and reactive power. The stator of DFIG is directly connected to grid and rotor is connected to the back to back power electronic convertor through slip rings when a disturbance occur in grid, therefore rotor cause high voltages which damages the converters connected to rotor and high voltage disturbances in the system. Due to high rotor inflow current, the over voltage and torque oscillations results damage of the doubly fed induction generator, this results the failure of rotor converters and mechanical parts [1]. To overcome this problem and to obtain an international standard grid code values called E.ON standards in olden days, the rotor crow bar circuit is connected to the rotor side converter [2-5]. The crow bar circuit is a series resistive network controlled by power electronics convertor. Crow bars care the rotor converters, when the grid disturbance is occurs it provides low resistance path to high rotor circuit and by pass the faculty rotor current, thereby it protect the rotor the rotor side converter from high voltages and current under grid disturbances but it converts doubly fed induction generator to squirrel cage induction generator, it consumes high reactive power from the grid. So turbines with crowbars is not efficient in maintaining grid codes, there is another disadvantage like equipment cost and it not decisive. To fulfill the new grid codes fault ride through capacity is crucial for DFIG. Many researchers have proposed different techniques to control this rather than using a crow bars, reference [6] proposed that the series resistance of current transformers on the rotor side could prevent rotor over current, thus preventing the rotor side converter from losing control over the generator. There are other proposed solutions from references [7-9] to achieve fault ride through the static synchronous compensator [STATCOM] and dynamic voltage restorer [DVR] are examined and compared. In reference [10] the current hysteresis PWM modulation technology in the moment of grid voltage change to achieve the suppression of rotor current. In reference [11] uses phase angle compensation technology to make the phase angle orientation of the control system move accurate during the grid voltage recovery, thus achieving the suppression of rotor current fluctuation, then the grid voltage drop is more serious, the above control strategy cannot remain DFIG in the safe operation state. At this time, the cascade crow bar device can be used to by bags and block the machine – side convertor [12] and the DC link of the convertor increases the chopper resistance to prevent DC over voltage [13], the machine-side convertor string resistance or DFIG's stator series resistance to avoid the convertor's short time out of control [14]. It is necessary to enhance the adaptability of the wind power system when the grid voltage drops by improving the control strategy. In order to solve these problems, some authors proposed a "demagnetization" control strategy [15]. To enhance the operation capability of DFIG under grid

faults, the authors in reference [16] proposed to improve the rotor current transient characteristics of power command step changes through virtual resistors. In reference [17] proposed a coordinated control strategy for a hybrid wind form with DFIG and Permanent magnet synchronous generator under symmetrical grid faults and the literature [18] proposes Improved demagnetization control of DFIG under balance grid faults, literatures [19-20] proposes low complexity model predictive direct power control for DFIG under both balance and unbalanced gird conditions. The literature [21] proposes scaled current tracking control for DFIG to ride through series grid faults. The literatures [22-23] proposes to suppress the high frequency resonance phenomenon between the DFIG system and a parallel compensated weak network, an active damping control strategy is introduced by inserting virtual impedance in to the stator branch with stator current feed forward control.

In the literature [24] a harmonic voltage control strategy based on a PIR regulator in d-q frame was proposed that used to suppress stator output voltage of a stand-alone DFIG system. In the literature [25] to achieve optimal control of harmonic voltage and current, a coordination factor is proposed to adjust the dynamic allocation for harmonic voltage and harmonic current at PCC. Here the aim of the paper is to control the DFIG at high currents in winding of rotor when faults occur in grid by using dynamic control of virtual resistance in the system. The whole system is controlled by the virtual resistance and demagnetization control.

2. Dynamic Analysis of DFIG during grid voltage disturbances.

The mathematical model of the double fed induction generator is first established to analyze the transient process during grid voltage dips. Usually the park model of the machine is used to analyze the behavior of DFIG. The equivalent circuit of the behavior at static – stator – oriented reference frame per phase from park model is shown in figure (1) [7,9].

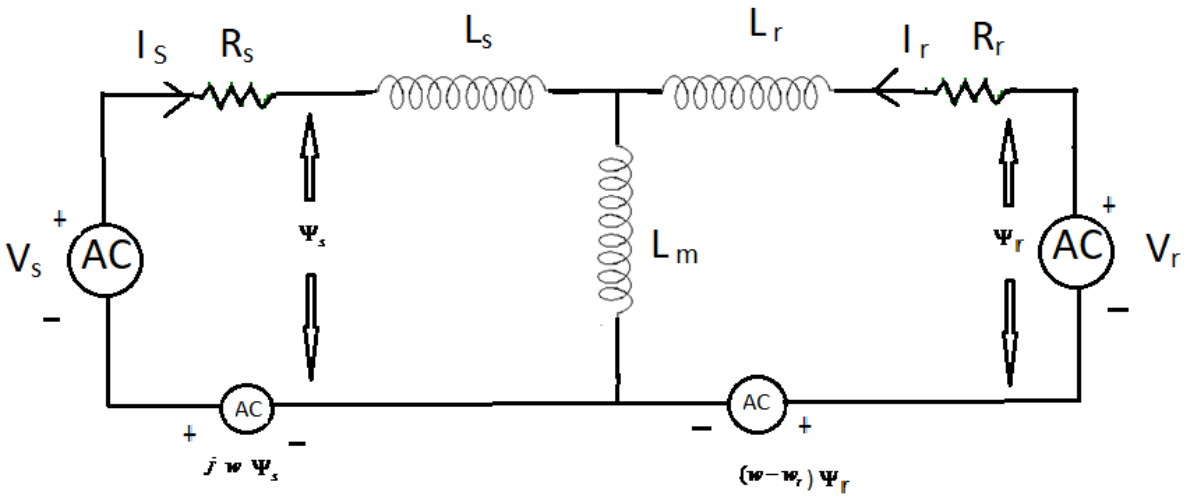

Fig.(1): Per phase equivalent circuit of DFIG in stator oriented reference frame

In the stationary coordinate system, the DFIG mathematical model expressed in vector form is from fig (1)

$$\Psi_s = L_s I_s + L_m I_r \quad (1)$$

$$\Psi_r = L_r I_r + L_m I_s$$

$$V_s = R_s I_s + \frac{d\psi_s}{dt} + j\omega\psi_s \quad (2)$$

$$V_r = R_r I_r + \frac{d\psi_r}{dt} + j(\omega - \omega_r)\psi_r \quad (3)$$

From the equations (1), (2), (3) we can obtain the rotor voltage as given below

$$V_r = \left[R_r + \sigma L_r \left(\frac{d}{dt} + j(\omega - \omega_r)\right)\right] I_r + \frac{L_m}{L_s}\psi_s\left[\frac{d}{dt} + j(\omega - \omega_r)\right] \quad (4)$$

$$V_r = \left[R_r + \sigma L_r\left(\mathrm{P} + j(\omega - \omega_r)\right)\right] I_r + \frac{L_m}{L_s}\psi_s[\mathrm{P} + j(\omega - \omega_r)] \quad (5)$$

Where $\sigma = \left(1 - \frac{L_m^2}{L_r L_s}\right)$ is the leakage factor

Where ω = stator speed of DFIG, so $\omega = 0$

Where = P is called P- operator

Now the equation (6) becomes

$$V_r = [R_r + \sigma L_r(\mathrm{P} - j\omega_r)] I_r + \frac{L_m}{L_s}\psi_s[\mathrm{P} - j\omega_r] \quad (6)$$

By introducing the leakage factor "σ" the rotor flux can be described as dependent of the rotor current and the stator flux.

The equation (6) consists of two parts. The first part is caused by the rotor current I_r and the second part is caused by the stator flux ψ_s that is given in normal operation by the constantly rotating vector.

$$\psi_s = \frac{V_s}{j\omega_s} e^{j\omega_s t} \quad (7)$$

Under the normal operating condition of DFIG the stator voltage is constant so, the stator flux is constant and under normal operating conditions, the stator resistance, rotor current and the leakage factor 'σ' is often small. So they are neglected under normal operating condition, the rotor voltage induced by the stator flux is expressed by modifying the equation (6) as follows:

$$V_r = \left[R_r + \sigma L_r \mathrm{P} + \mathrm{j}\sigma \mathrm{L_r}\,\psi_{\mathrm{slip}}\right] I_r + \frac{L_m}{L_s} \mathrm{s} V_s e^{j\omega_s t} \quad (8)$$

$$V_r = \left[R_r + \sigma L_r \mathrm{P} + \mathrm{j}\sigma \mathrm{L_r}\,\psi_{\mathrm{slip}}\right] I_r + \frac{L_m}{L_s} \mathrm{s}\bar{v_s} \quad (9)$$

The rotor voltage induced by the stator flux increases at the instant of full symmetrical stator dip. Under a symmetrical voltage dip the stator side voltage is reduced from normal amplitude V_{s1} to the faulty amplitude V_{s2} as described in equation (8)

At the time instant t = t_0, a fault appears in the grid, and the corresponding stator side voltage is expressed as

$$\overline{V_s} = \begin{cases} v_{s1} e^{jw_s t} & \text{for } t \le t_0 \\ v_{s2} e^{jw_s t} & \text{for } t \ge t_0 \end{cases} \quad (10)$$

And the flux linkages

$$\overline{\Psi_s} = \begin{cases} \overline{\Psi_{s1}} = \frac{v_{s1}}{jw_s} e^{jw_s t} & \text{for } t \le t_0 \\ \overline{\Psi_{s2}} = \frac{v_{s2}}{jw_s} e^{jw_s t} & \text{for } t \ge t_0 \end{cases} \quad (11)$$

The evolution of the stator flux can be derived by solving the differential equation (12) [from equations (1) & (2), assuming $\overline{ir} = 0$, due to its low influence on the rotor voltage).

$$\frac{\overline{d\psi_s}}{dt} = \overline{V}_s - \frac{R_s}{L_s}\overline{\psi}_s \quad (12)$$

The solution consists of two parts. The first part is the steady state stator flux after the voltage dip that is denoted by $\overline{\Psi_{s2}}$ and the second part is the transition of the flux from $\overline{\Psi_{s1}}$ to $\overline{\Psi_{s2}}$ that is described equation (13)

$$\bar{\psi}_s = \bar{\psi}_{s0} e^{\frac{-Rt}{L}} = \bar{\psi}_{s0} e^{\frac{-t}{T}} \quad (13)$$

Where $\overline{\Psi_{s0}}$ the different of the stator is flux before and after the voltage dip, described by $(v_{s1} - v_{s2})/jw_s$, summarizing, and the stator flux is given by the sum of the two parts.

$$\bar{\psi}_s(t) = \frac{V_{2s}}{j\omega_s} + \frac{V_{1s} - V_{2s}}{j\omega_s} e^{-\frac{t}{T}} \quad (14)$$

When the dynamic stator flux from equation (14) is considered in the rotor voltage equation of (6) (neglecting i_r and $1/T_s$), the dynamic behavior of the rotor voltage under symmetrical voltage dip is described as

$$v_r = \frac{L_m}{L_s}\left(\frac{d}{dt} - jw\right)\left(\frac{v_{s2}}{jw_s} e^{jw_s t} + \frac{v_{s1} - v_{s2}}{jw_s} e^{-t/T_s}\right)$$

If the reference frame is rotating at rotor frequency, the following rotor voltage is obtained

$$V_r = \frac{L_m}{L_s}(sV_{s2} e^{j\omega_s t} - (1-s)(V_{s1} - V_{s2} e^{-j\omega_s t} e^{\frac{-t}{T}}) \quad (15)$$

The rotor voltage equation (15) during symmetrical voltage dip consists of two components. The first part is proportional to the slip and the remaining depends on stator voltage, thus for a deep voltage dip and a slip usually at 0.2 to 0.5, it is very small. The first part of the equation (15) is slip frequency, and the second part of equation (15) has a high amplitude at t = 0 proportional to (1-s) and rotates at the electrical rotor frequency. The part is decaying exponentially with the stator time constant of "T".

3. Proposed Technique

3.1 Dynamic virtual resistance control

From equation (6) the equivalent circuit of DFIG at rotor side, under grid disturbance can be obtained as shown in fig. 2

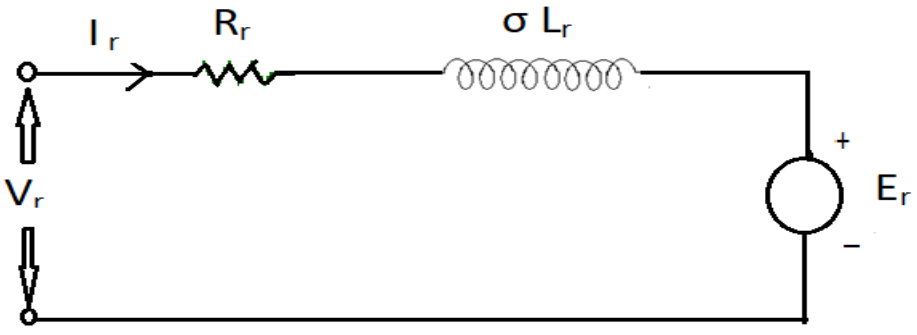

Fig (2): Equivalent circuit diagram viewed from rotor side

The virtual resistance control strategy is used to enhance the voltage stability and improve the fault ride through (FRT) and suppress the oscillation of DFIG during grid voltage disturbance.

From the equation (6) and the equivalent DFIG model shown in the fig (2), the inner current loop of the DFIG is shown in fig. 3.

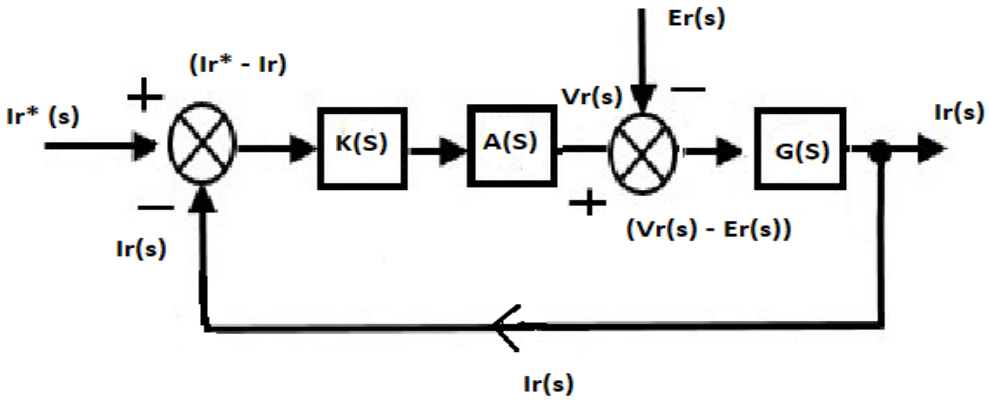

Fig. (3) – Control block diagram of DFIG inner current loop

To calculate the total gain G(s) value from equivalent circuit fig. 2 we get

$$G(s) = \frac{\frac{1}{R_r}}{1+\sigma\frac{sL_r}{R_r}}$$

$$G(s) = \frac{K_1}{1+SK_2} \quad (16)$$

$$K_1 = \frac{1}{K_r}, K_2 = \sigma L_r / R_r$$

Now consider DFIG inner current loop block diagram with dynamic virtual resistance. The fig. (4) Shows, the equivalent DFIG circuit viewed from rotor side

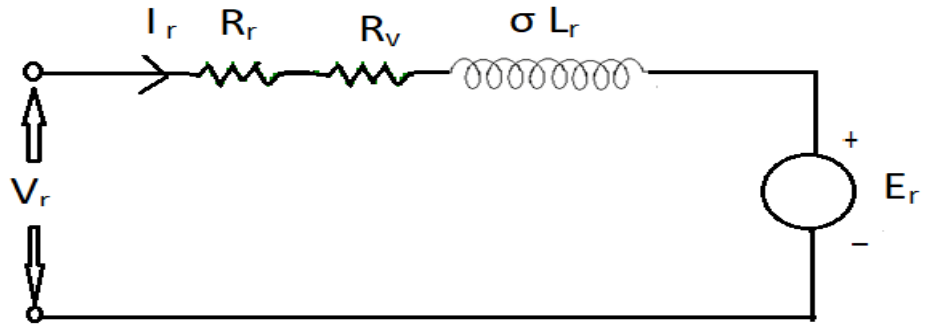

Fig. (4) Equivalent DFIG Model viewed from rotor side after introducing virtual resistor

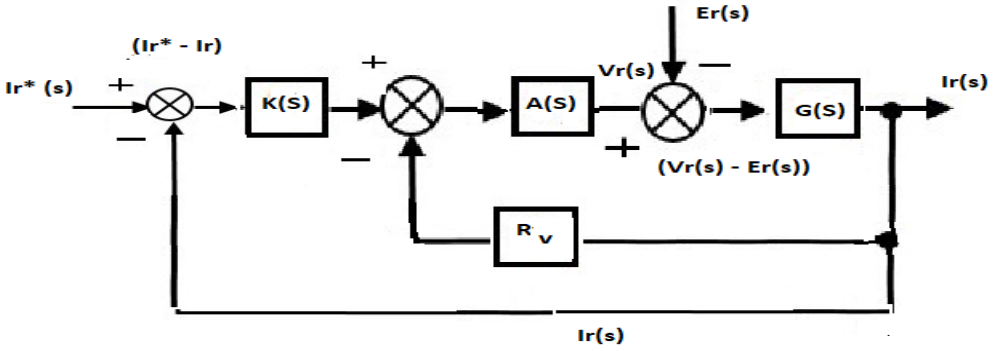

Fig. (5): Control block diagram of DFIG inner loop after introducing virtual resistance

To calculate the total gain G(s) value from equivalent circuit fig. 4 we get

$G^{I}(s) = \frac{K_1}{1+SK_2}$ (17)

Where $K_1 = \frac{1}{R_v+R_r}$, $K_2 = \frac{\sigma L_r}{R_r+R_v}$

Comparing G(s) and $G^{I}(s)$ from equations (16) & (17), it can be seen that after the introduction of the virtual resistor, the time constant is reduced by $\frac{1}{R_v + R_r}$ times Therefore, the inertia of the controlled object of the current inner loop after the addition of the virtual resistor is reduced.

3.2. Selection of Virtual Resistance value

The rotor voltage equation after introducing the virtual Resistance in the rotor coordinate system is given

$V_r = \left[R_V + R_r + \sigma L_r \left(\frac{d}{dt} - j\omega_r\right)\right] I_r + \frac{Lm}{L_s}\psi_s[\frac{d}{dt} - j\omega_r]$ (18)

Now above equation can modified and the value of the virtual resistance can be expressed as

$$R_V = \left(\frac{V_{r-E_r}}{I_r}\right) - \sqrt{{R_r}^2 + {X_r}^2}$$

$$R_V = |\Delta V| - \sqrt{{R_r}^2 + {X_r}^2} \quad (19)$$

$E_r = \frac{Lm}{L_s}\psi_s[\mathrm{P} - j\omega_r]$

Where $|\Delta V| = \left(\frac{V_r - E_r}{i_r}\right)$

I can be seen from equation (19) that although the control method can inhibit the oscillation of the rotor current when power grid voltage changes to abnormal, the DFIG rotor side damping is improved, but as the rotor electromotive force increases, the rotor side voltage also increases. Since the DFIG voltage is related to the motor speed and the grid voltage drops degree, it is necessary to select a suitable virtual resistor to ensure that the rotor current oscillation is suppressed and the voltage is not too high, and the transient time is not lengthened under a certain speed a grid voltage dips.

According to the equation (15), the rotor side indication electromotive force is related to the slip rate and the degree of voltage drop. When the voltage dips, when the DFIG runs in the super – synchronous state (S<0) the degree of voltage drops increases and the induction electromotive force of rotor side increases accordingly. In order to ensure the normal operation of the rotor-side, converter, the required rotor excitation voltage also increases. In this case, the rotor virtual

resistance is too large to cause the rotor side over voltage, so the virtual resistance value should change with the voltage drop depth, to meet the stable operation of the double fed fan during the fault when the voltage drop is small at this time, there is a margin in the rotor side voltage and a larger virtual resister selected; When the grid voltage drop is large, a smaller virtual resistor is selected. According to the design goal the maximum voltage drop of the normal operation can be controlled by the voltage dip of 30% and the range of the virtual resistance of the voltage drop in the range of 0 – 20% is as follows:

$$\left|\frac{V_{rmax}-E_{xp-20\%}}{I_{rmax}}\right| - \sqrt{{R_r}^2 + {X_r}^2} \leq R_V \leq \left|\frac{V_{rmax}-E_{xp-0\%}}{I_{rmax}}\right| - \sqrt{{R_r}^2 + {X_r}^2} \quad (20)$$

In equation (20) 'P' represents the degree of voltage drops when, the voltage drops are 20%, the minimum value of the virtual resistance is obtained. When the voltage drops to '0' zero, that is in the stable operation state, the maximum value of the virtual resistance is obtained, at this time, the current is the rated current. The rotation between the virtual resistance and the voltage drop is follows.

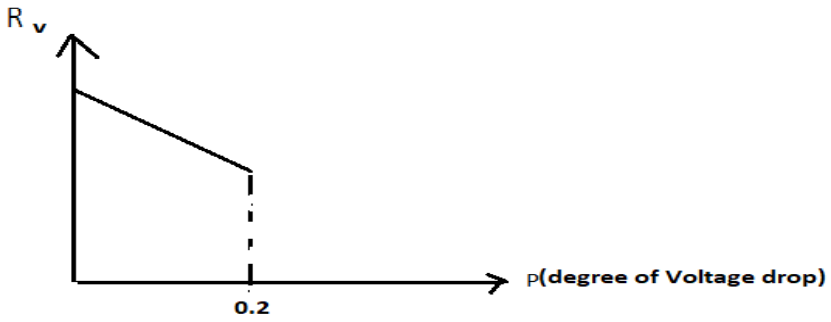

Fig. (6) Degree of voltage drops

According to Fig (6), dynamic virtual resistance can be expressed as $R_v = Kp + R_{max}$, according to the formula.

The value of the dynamic virtual resistance can be obtained under different voltage drop degrees. As the grid voltage dips increases, the virtual resistance decreases monotonically to achieve to rotor voltage is limited within the maximum allowable voltage range, the current oscillation caused by the fault is rapidly attenuated.

4. Control Strategy:

The enhanced control strategy is introduced to decrease the currents of rotor at grid during a voltage dip, the developed control technique is having space vector pulse width modulation controller, voltage dip detector, LVRT controller PLL, virtual resistance controller. In switching normal controller to the LVRT controller, quick detection of fault at grid is important. The voltage dips are of two types, symmetric dip and asymmetric dip. Symmetric dip contains a positive component in the stator voltage, so the wind generator system is a s-line and s-ϕ system and the detection of voltage dip at symmetric dip can detected by converting 3ϕ voltage variable in a common reference frame to a synchronous d-q reference frame. The converted d-q variables are corresponding to the magnitude of the stator voltage, so comparing with the values of d-q variables when voltage dip is zero and with voltage dip, voltage dip can be detected. Similarly in asymmetric sag it consists of positive component and negative components in the stator voltage, the new d-q variables consists a second order ac harmonic component with a dc component.

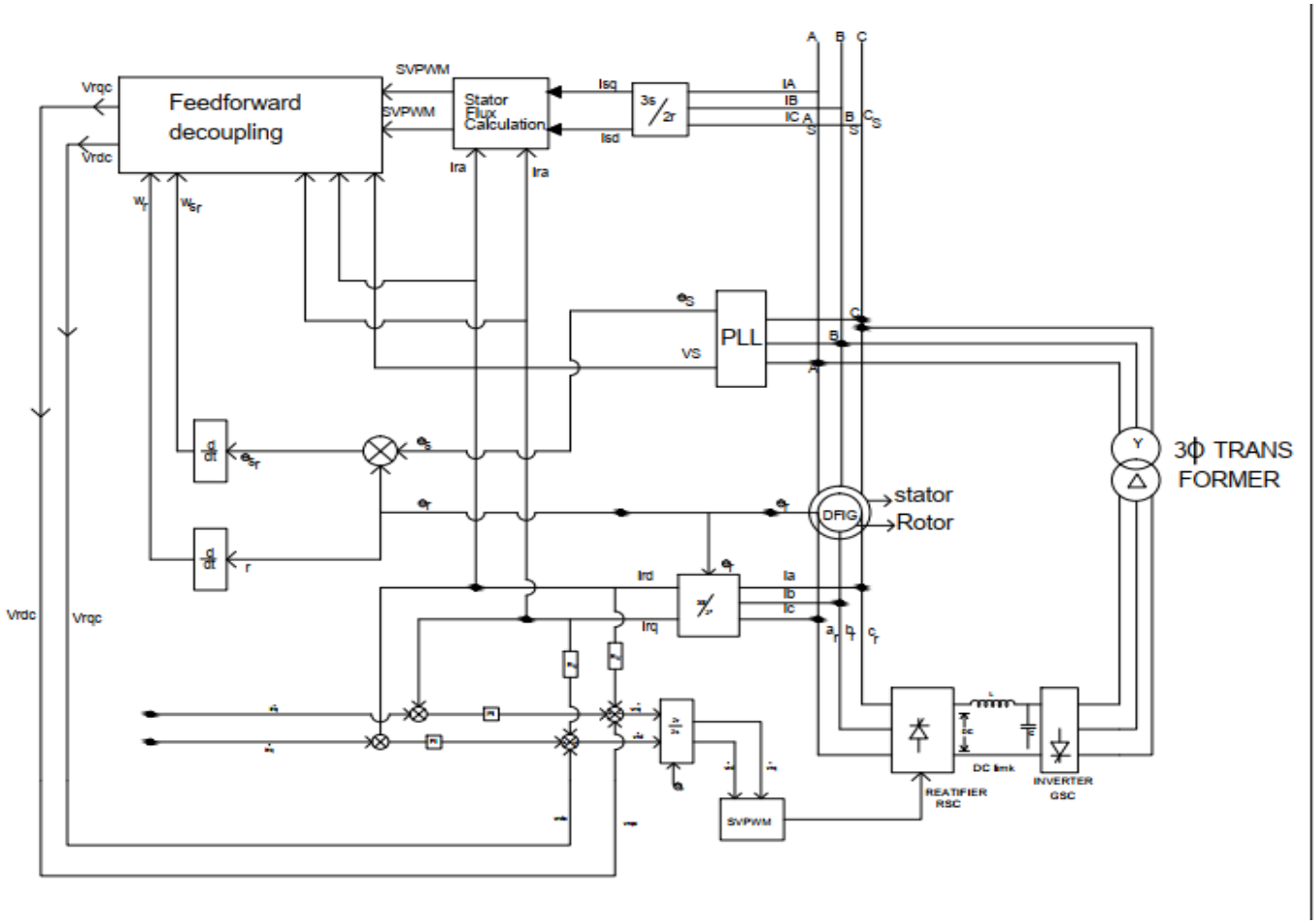

FIGURE (7): BLOCK DIAGRAM OF DFIG CONTROL SYSTEM BASED ON VIRTUAL RESISTANCE SCHEME

5. Simulation Results

To analyze the effect of dynamic virtual resistance control, for grid voltage vaults, this paper takes the 3KW DFIG as the research object and carries out the simulation research using "SIMULINK" DFIG parameter: Stator rotated voltage is 440V, stator rated current 20A, rotor open circuit voltage is 300 V, pole logarithm is 1.5, stator inductance "L_s" is 0.05pu, rotor inductance "L_s" is 0.025 pu. Mutual inductance L_m is 1.2 pu, rotor resistance "R_r" is "0.002pu" and the stator resistance is 0.0015pu. The following figures show that the voltage drop is 20%, 15% and the fault start time is 0.5 sec. Under the conventional control scheme, the dynamic virtual resistance control scheme and the fixed virtual resistance control, the rotor current d-q axis component, and the rotor voltage shown in fig. is (8) & (9).

After the addition of the virtual resistor, the rotor current shock caused by the sudden voltage drop of the grid is well suppressed. Taking the voltage drop of 20% as an example, the rotor current impact caused by the dynamic virtual resistance is 86.8% of the rotor in rush current under conventional control. After adding the virtual resistor, the rotor voltage will increase. Because the value of the virtual resistor is different under different voltage drops, the rotor voltage does not exceed the maximum capacity of the rotor side convertors.

Compared with the fixed resistance value, the control method of the dynamic virtual resistance weakness the suppression of the rotor current, but the generated rotor voltage impact value is smaller, which satisfies the purpose of the rotor side not being over pressures the resistance value is a fixed resistor, although the resistance value is a fixed value, the rotor current oscillation can be suppressed.

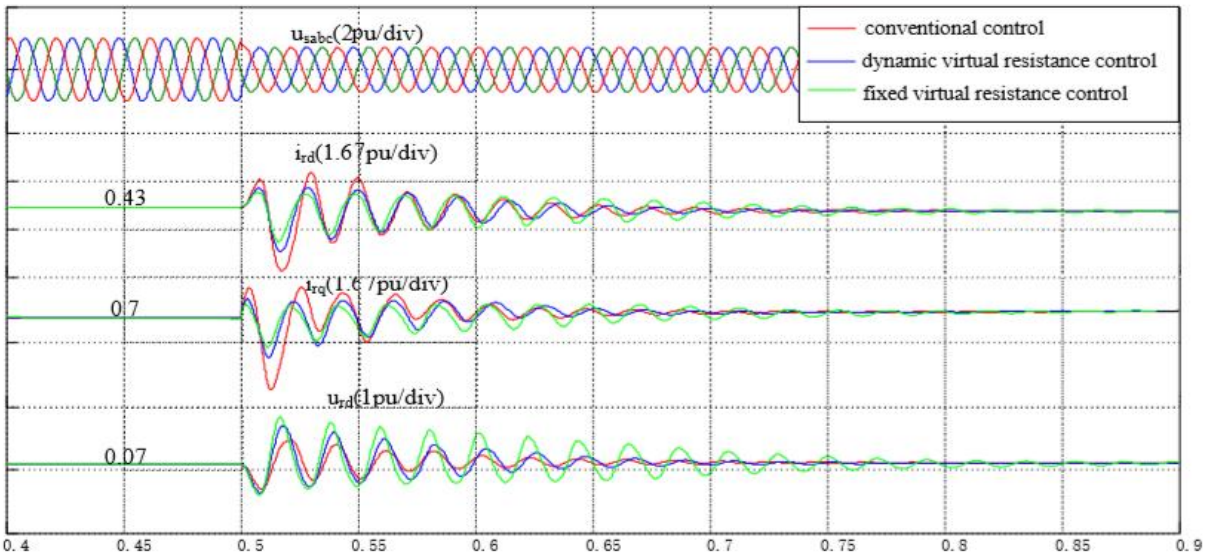

Figure (8). Experimental results with 20% stator voltage sag

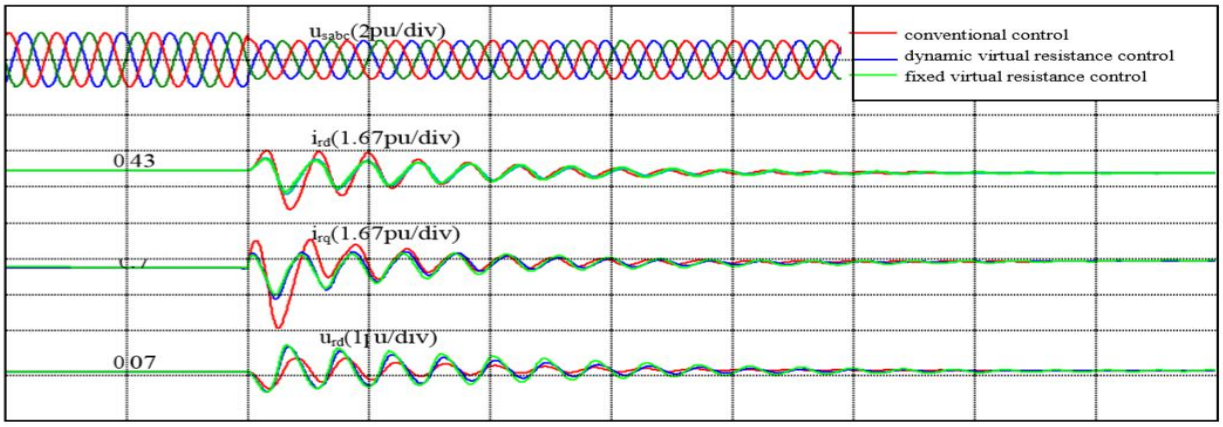

Figure (9). Experimental results with 15% stator voltage sag

6. Conclusion

In this paper, the transient process of DFIG under the symmetrical faults of grid voltage is analyzed. The dynamic virtual resistance control scheme is proposed, and the calculation method of dynamic virtual resistor is given. The control method can effectively suppress the rotor current oscillation under different degrees of voltage drops, and avoid the rotor side overvoltage. Finally, the simulation analysis proves the correctness and effectiveness of the proposed control strategy.

7. References

[1] Lopez, J.; Sanchis, P.; Roboam, X.; Marroyo, L. "Dynamic behavior of the doubly fed induction generator during three-phase voltage dips". IEEE Trans. Energy Convers. 2007, 22, 709.

[2] Duong, M.Q.; Le, K.H.; Grimaccia, F.; Leva, S.; Mussetta, M.; Zich, R. "Comparison of power quality in different grid-integrated wind turbines". In Proceedings of the 2014 16th International Conference on Harmonics and Quality of Power (ICHQP), Bucharest, Romania, 25–28 May 2014; pp. 448–452.

[3] Sava, G.N.; Costinas, S.; Golovanov, N.; Leva, S.; Duong, M.Q."Comparison of active crowbar protection schemes for DFIGs wind turbines". In Proceedings of the 2014 16th International Conference on Harmonics and Quality of Power (ICHQP), Bucharest, Romania, 25–28 May 2014; pp.669–673.

[4] Duong, M.Q.; Grimaccia, F.; Leva, S.; Mussetta, M.; Sava, G.; Costinas, S. "Performance analysis of grid-connected wind turbines". UPB Sci. Bull. C Electr. Eng. 2014, 76, 169–180.

[5] Fortmann, J.; Pfeiffer, R.; Haesen, E.; van Hulle, F.; Martin, F.; Urdal, H.; Wachtel, S. "Fault-ride- through requirements for wind power plants in the ENTSO-E network code on requirements for generators". IET Renew. Power Gener. 2014, 9, 18–24.

[6] Duong, M.Q.; Nguyen, H.H.; Le, K.H.; Phan, T.V.; Mussetta, M. "Simulation and performance analysis of a new LVRT and damping control scheme for DFIG wind turbines". In Proceedings of the 2016 IEEE International Conference on Sustainable Energy Technologies (ICSET), Hanoi, Vietnam, 14–16 November 2016; pp. 288–293.

[7] H. Geng.; C. Liu.; and G. Yang.; "LVRT capability of DFIG- based WECS under asymmetrical grid fault condition," IEEE Transactions on Industrial Electronics, 2013, vol. 60, no. 6, pp. 2495– 2509.

[8] J. P. da Costa.; H. Pinheiro.; T. Degner.; and G. Arnold.; "Robust controller for DFIGs of grid- connected wind turbines," IEEE Transactions on Industrial Electronics, 2011, vol. 58, no. 9, pp. 4023– 4038

[9] N.Patin.; E.Monmasson.; and J.-P.Louis.; "Modeling and control of a cascaded doubly fed induction generator dedicated to isolated grids," IEEE Transactions on Industrial Electronics, 2009, vol. 56, no. 10, pp.4207–4219.

[10] Mohseni M.; Islam S M.; And Masoum M A S.; "Fault ride-through capability enhancement of doubly-fed induction wind generators", IET Renewable Power Generation.2011, 5 (5) 368-376.

[11] WANG Wei.; CHEN Ning.; and ZHU Lingzhi.;. "Phase angel compensation control strategy for low-voltage ride through of doubly-fed induction generator", Proceedings of the CSEE, 2009, 29 (21) 62-68.

[12] Hansen A.D.; And Michalke G.; "Fault ride-through capability of DFIG wind turbines", Renewable Energy, 2007, 32 (9) 1594-1610.

[13] Martinez J.; Kjar P C.; and Rodriguez P.; "Parameterization of a synchronous generator to represent for fault studies", Wind Energy, 2011, 14 (1) 107-118.

[14] YANG J.; Fletcher E.; and O Reilly J.; "A Series dynamic resistor based converter protection scheme for doubly-fed induction generator during various fault conditions", IEEE Transactions on Energy Conversion, 2010, 25 (2) 422-432. s

[15] Xiang D.; Ran L.; and Tavener P J.; "Control of a doubly fed induction generator in a wind turbine during grid fault ride-through", IEEE Transaction on Energy Conversion, 2006, 21 (3) 652- 662.

[16] Petersson A.; Harnefors L.; and Thiringer T.; "Evaluation of current control methods for wind turbine using doubly-fed induction machines", IEEE Transactions on Power Electronics, 2005,20 (1) 227-235.

[17] Li, J.; Yao, J.; Zeng, X.; Liu, R.; Xu, D.; Wang, C.; "Coordinated Control Strategy for a Hybrid Wind Farm with DFIG and PMSG under Symmetrical Grid Faults". Energies 2017, 10, 669.

[18] Zhou, L.; Liu, J.; Zhou, S.; "Improved demagnetization control of a doubly-fed induction generator under balanced grid fault". IEEE Trans. Power Electron. 2015, 30, 6695–6705.

[19] Sun, D.; Wang, X., "Low-Complexity Model Predictive Direct Power Control for DFIG under Both Balanced and Unbalanced Grid Conditions"., IEEE Trans. Ind. Electron, 2016, 63, 5186– 5196.

[20] Song, Y.; Nian, H.; "Modularized control strategy and performance analysis of DFIG system under unbalanced and harmonic grid voltage", IEEE Trans. Power Electron, 2015, 30, 4831– 4842.

[21] Huang, Q.; Zou, X.; Zhu, D.; Kang, Y.; "Scaled Current Tracking Control for Doubly Fed Induction Generator to Ride-Through Serious Grid Faults",IEEE Trans. Power Electron, 2016, 31, 2150–2165.

[22] Song, Y.; Wang, X.; Blaabjerg, F.; "Doubly Fed Induction Generator System Resonance Active Damping through Stator Virtual Impedance", IEEE Trans. Ind. Electron, 2017, 64, 125–137.

[23] Song, Y.; Wang, X.; Blaabjerg, F.; "High-Frequency Resonance Damping of DFIG-Based Wind Power System Under Weak Network", IEEE Trans. Power Electron, 2017, 32, 1927– 1940.

[24] Phan, V.; Lee, H; "Control Strategy for harmonic elimination in stand-alone DFIG applications with nonlinear loads",IEEE Trans. Power Electro,. 2011, 26, 2662–2675.

[25] Zhen Xie.; Lifan Niu.; and Xing Zhan.; "An Enhanced Control Strategy for Doubly-Fed Induction Generators Based on a Virtual Harmonic Resistor and Capacitor under Nonlinear Load Conditions", Energies, MPDI, open Access Journal, October 2018, vol, 11(5),pages 1-7

Nomeneculture

V_r & V_s represent rotor and stator voltages respectively

R_s & R_r represent stator and rotor resistances respectively.

i_s & i_r represent stator and rotor currents respectively.

ψ_r & ψ_s represent rotor and stator flux linkage respectively.

L_s & L_r represent stator and rotor inductance respectively.

L_m = mutual inductance between stator and rotor.

w_r = represent the rotor angular velocity

Where $w_{s1} = w_s - w_r$

slip (s) = $\frac{w_{s2}}{w_s} = \frac{w_s - w_r}{w_s}$

w_s = machine angular velocity of field in the machine

K(s) = Transfer function of current regulator = $K_p + K_i/s$

A(s) = Transfer function of rotor regulator = K_t

G(s) = Transfer function of DFIG according to inner current loop

R_v = Virtual Resistance

R_r = Rotor Resistance

L_r = Rotor Inductance

E_r = Rotor EMF due to stator fulx

SVPWM = space vector pulse width modulation

PI= proportional integral controller

Author's Profile

a : S.RAJESH

He is graduated in Electrical& Electronics Engineering from Jawaharla Nehru Tecnological University, Hyderabad in 2006, and received M.Tech in Power Electronics from JNTUH, in 2010; presently he is pursuing his Ph.D in Electrical Engineering at Osmania University Hyderabad. He is life member of Indian society for Technical Education (ISTE) and International Association of Engineers (IAENG) His areas of interest in Applications of Power electronics converters in renewable Energy sources, wind energy generation

b : Dr.P.Venkata Prasad

He is currently working as professor in the department of and electronics engineering in Chaithanya Bharathi Institute of Technology, Hyderabad .He was former Head of the department of EEE. He has 20 years of Experience in teaching. He has published around 70 research papers in International and National Journals and Conferences. He has also authored for text books in Electrical Engineering. He has received best Teacher award in CBIT. He is senior member of IEEE and FIE. His areas of interest include power system optimization, power quality, smart grid Electrical Distribution Optimization ect.

c : Dr.P.Srinivas

He is graduated in Electrical and Electronics Engineering from Kakatiya University, Warangal in 1998 and received M.Tech in Electrical Machine & Industrial Drives from National Institute of Technology, Warangal in 2000. Presently he is serving as Professor in the department of Electrical Engineering in Osmania University. He is received his Ph.D in Electrical Engineering from Osmania University in 2013.He is also lif member of many professional bodies. His areas of interest are Special Electrical Machines, AI Techniques to Electrical Drives. He has got eleven National and International papers and presented a technical paper in seoul, south Korea in 2007